NASA TECHNICAL NOTE

NASA TN D-4700

NASA TN D-4700

C. 1

COLD-AIR INVESTIGATION OF EFFECTS OF PARTIAL ADMISSION ON PERFORMANCE OF 3.75-INCH MEAN-DIAMETER SINGLE-STAGE AXIAL-FLOW TURBINE

by Hugh A. Klassen

Lewis Research Center
Cleveland, Ohio

NATIONAL AERONAUTICS AND SPACE ADMINISTRATION • WASHINGTON, D. C. • AUGUST 1968

COLD-AIR INVESTIGATION OF EFFECTS OF PARTIAL ADMISSION ON PERFORMANCE OF 3.75-INCH MEAN-DIAMETER SINGLE-STAGE AXIAL-FLOW TURBINE

By Hugh A. Klassen

Lewis Research Center
Cleveland, Ohio

NATIONAL AERONAUTICS AND SPACE ADMINISTRATION

For sale by the Clearinghouse for Federal Scientific and Technical Information
Springfield, Virginia 22151 – CFSTI price $3.00

ABSTRACT

Total to static efficiency is described as a function of percentage of admission and blade-jet speed ratio. At design blade-jet speed ratio, efficiency decreased from 0. 68 to 0. 56 as percentage of admission was reduced from 100 to 11. 76. Partial admission efficiency losses are divided into rotor pumping and windage losses and all other losses.

STAR Category 03

COLD-AIR INVESTIGATION OF EFFECTS OF PARTIAL ADMISSION ON PERFORMANCE OF 3.75-INCH MEAN-DIAMETER SINGLE-STAGE AXIAL-FLOW TURBINE

by Hugh A. Klassen

Lewis Research Center

SUMMARY

An experimental investigation was conducted to determine the effects of partial admission operation on the performance of a 3.75-inch (9.52-cm) mean-diameter turbine. The tests, conducted in cold air, covered admission values of 100, 51, 31, and 12 percent. The partial admission losses were divided into rotor pumping losses and all other losses.

The efficiency decreased as the percentage of admission was reduced. At approximately design blade-jet speed ratio, the static efficiency decreased from 0.68 to 0.56 as admission was reduced from 100 to 12 percent. From the assumption that rotor pumping and windage losses are proportional to the percentage of inactive arc, all other partial admission losses were determined to be essentially constant. These other losses corresponded to a static-efficiency decrease of approximately 4 points for all test conditions.

Stator discharge pressures were highest at the edge of the arc of admission where the rotor blades first entered the active flow area. These high pressures may have been caused by scavenging losses.

INTRODUCTION

In the design of low-volume-flow, single-stage turbines, tip clearance losses and low blade-jet speed ratios resulting from small diameters can have significant effects on performance. The partial admission design, in which flow is admitted through only a fraction of the stator annulus, allows freedom to increase blade height and wheel diameter. Tip clearance losses are reduced and blade-jet speed ratio is increased. Partial admission, however, introduces other losses which tend to offset gains in performance.

This investigation was conducted to obtain an understanding of the effects of partial admission operation on the performance of a small-diameter, axial-flow turbine. The performance of a 3.75-inch (9.52-cm) mean-diameter turbine was investigated in cold air for admission values of 100, 50.98, 31.37, and 11.76 percent. This report presents the results of the cold-air investigation together with an analysis of the partial admission losses.

TURBINE DESCRIPTION

Design Requirements and Operating Conditions

The design requirements and operating conditions for the 3.75-inch (9.52-cm) mean-diameter, single-stage, axial-flow turbine were as follows (all symbols defined in appendix A):

Overall equivalent specific-work output, $\Delta h/\theta_{cr}$, Btu/lb; joule/g	21.8; 50.8
Blade-jet speed ratio, ν	0.377
Equivalent weight flow, $W\sqrt{\theta_{cr}}\,\epsilon/\delta$, lb/sec; kg/sec	0.060; 0.0222
Speed-work parameter, λ	0.44
Equivalent mean-section blade velocity, $U_m/\sqrt{\theta_{cr}}$, ft/sec; m/sec	490.9; 149.6
Equivalent speed, $N/\sqrt{\theta_{cr}}$, rpm	30 000
Total to static efficiency, η_s	0.645
Reaction across rotor, R	0
Overall total- to static-pressure ratio, p_2'/p_4	3.030
Stator total- to static-pressure ratio, p_2'/p_3	2.243
Admission, percent	31.37

Velocity Diagrams and Blade Design

The design free-stream velocity diagrams and blade profiles are shown in figure 1. The stator-outlet velocity is slightly supersonic with a critical velocity ratio $\left(V/V_{cr}\right)_3$ of 1.080. The rotor-inlet and rotor-outlet critical velocity ratios $\left(W/W_{cr}\right)_3$ and $\left(W/W_{cr}\right)_4$ have equal values of 0.666. Design turning in the rotor is 123.39°. Exit whirl is slightly negative. The actual stator throat area is 2.2 percent less than the design value. This difference should result in a higher stator-outlet velocity and a lower reaction across the rotor than indicated by the design velocity diagrams.

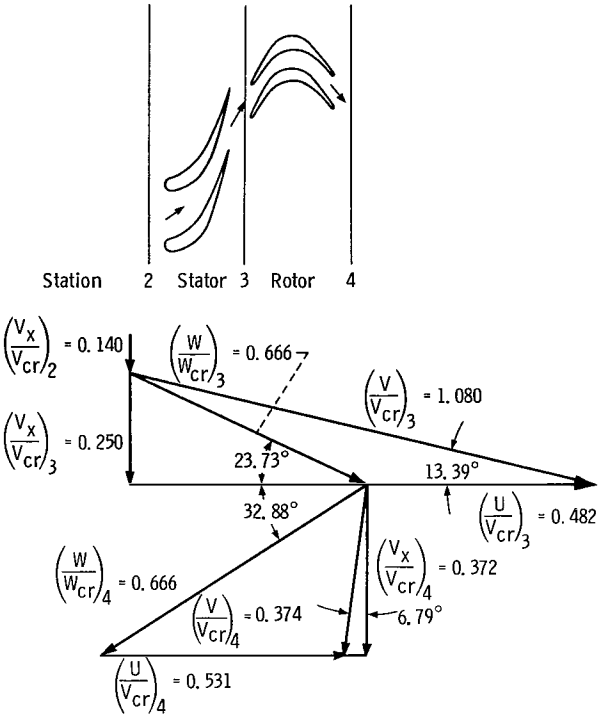

Figure 1. - Blade profiles and free-stream velocity diagrams.

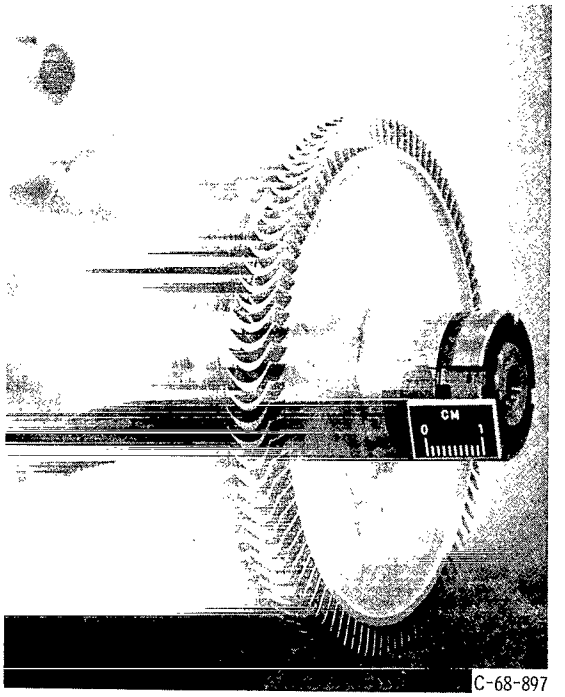

Figure 2. - Rotor.

TABLE I. - BLADE DESIGN INFORMATION

	Stator	Rotor
Admission, percent	31.37	------
Number of blades	16	95
Blade height,		
in.	0.217	0.226
cm	0.551	0.574
Chord,		
in.	0.453	0.312
cm	1.15	0.792
Solidity	1.96	2.52
Aspect ratio	0.48	0.72
Stagger angle, deg	59.2	7.1
Trailing edge radius,		
in.	0.0024	0.0025
cm	0.0061	0.0064
Leading edge radius,		
in.	0.0196	0.0050
cm	0.0498	0.0130

The rotor is shown in figure 2. Design information for the stator and rotor blading is given in table I.

APPARATUS, INSTRUMENTATION, AND PROCEDURE

The following apparatus was used in this investigation: the turbine assembly; an airbrake to absorb and measure the power output of the turbine; air supplies for the turbine, the turbine bearings, and the airbrake; and a vacuum exhaust system.

The turbine assembly included the rotor and the stator together with the appropriate inlet and exhaust ducting. The rotor was mounted on gas-lubricated bearings to minimize friction torque. The two journal bearing sleeves were fully cylindrical with eight equally spaced orifices for external pressurization. Thrust was absorbed with a double-

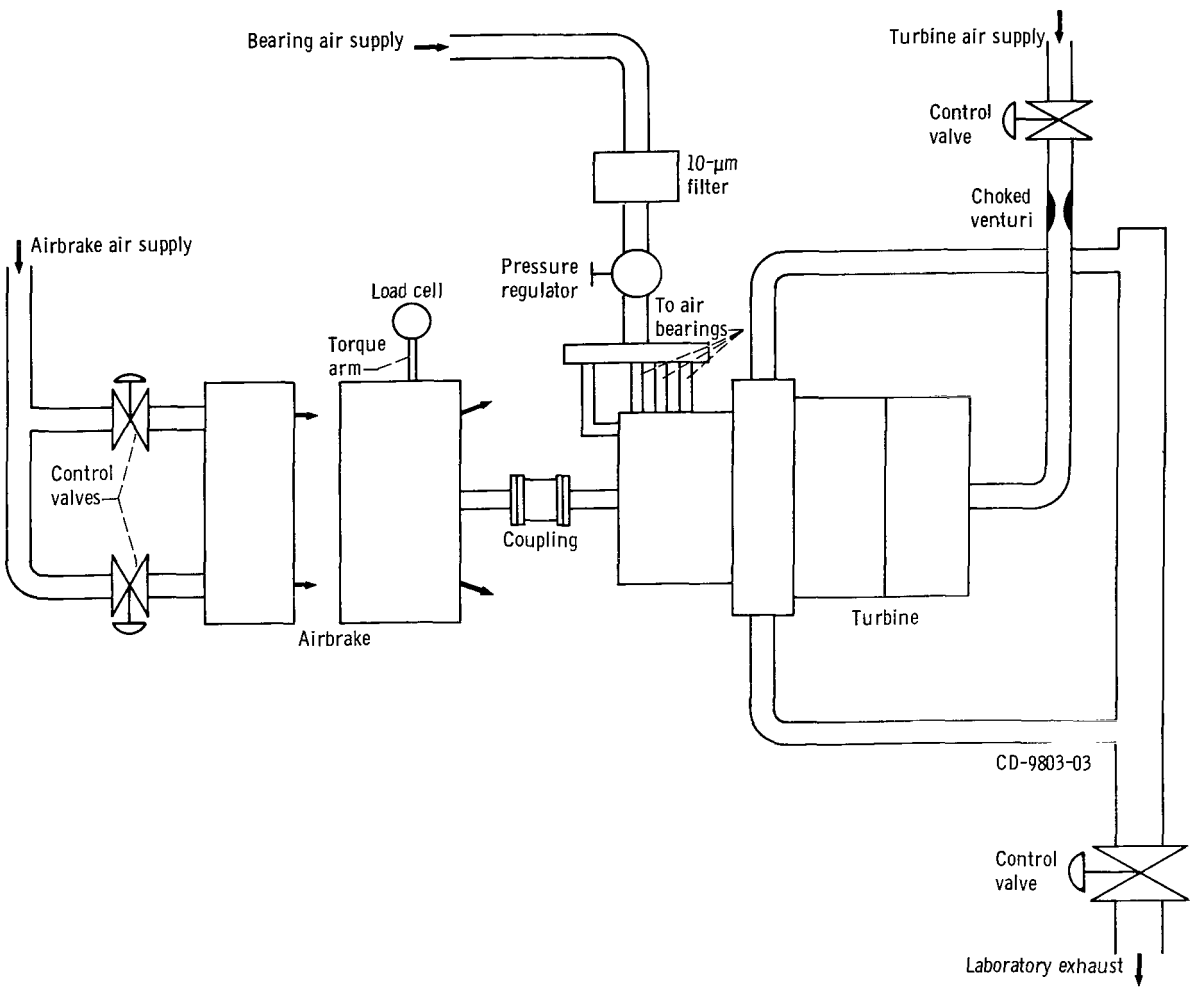

Figure 3. - Schematic diagram of test apparatus.

acting thrust bearing. The thrust runner was a plain disk, and the two thrust stators each had six recessed orifices for external pressurization.

A schematic diagram of the facility, showing the apparatus, is presented in figure 3. Dry pressurized air was supplied to the turbine inlet through a pressure control valve. Turbine weight flow was measured by a venturi operating under supercritical conditions. Two venturis of different throat diameters were used. The smaller venturi was used only for the 12 percent admission test. Turbine-outlet flow passed through a control valve to the laboratory vacuum exhaust system.

The turbine measuring stations are shown in figure 4. Turbine-inlet total temperatures were measured by two thermocouples in the inlet collector (station 1). All static-pressure measurements were taken at the outer wall except for stator-inlet static pressure, which was measured at the inner wall. Data obtained during a previous investigation showed that the pressure difference between hub and tip is negligible for both the stator and rotor. The pressure variation between hub and tip is small because of the high hub-tip radius ratio. Stator-inlet static pressure p_2 was measured at station 2 with four taps, two in the arc of admission and two in the inactive region. Stator-inlet

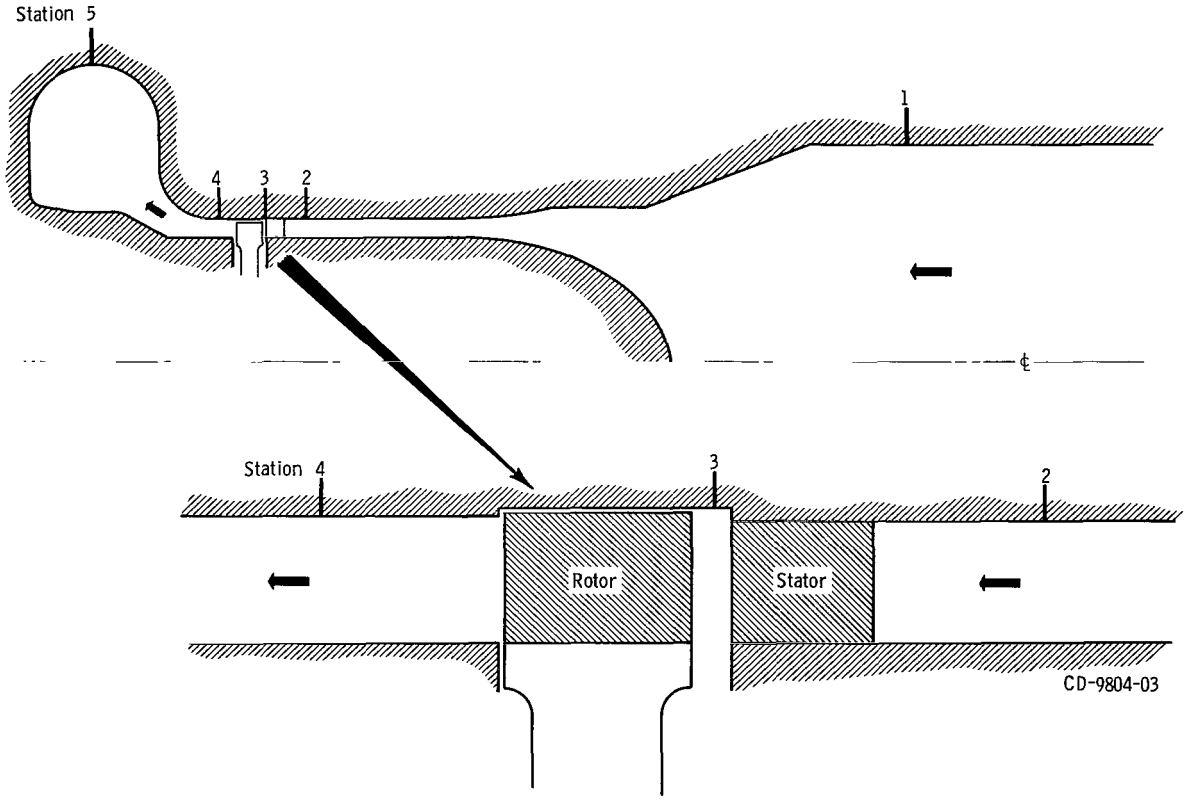

Figure 4. - Flow passage and turbine measuring stations.

total pressure p'_2 was computed from the measured static pressure for the active portion of the stator, the turbine-inlet total temperature, the weight flow, and the active portion of the annulus area. Stator-outlet static pressure p_3 was measured with six taps. For admission values of 100 and 31 percent, all six taps were in the arc of admission. For 51 percent admission, three were in the arc of admission, and for 12 percent admission, only two taps were in the arc of admission. Rotor-outlet static pressure p_4 was measured with four taps. Two of these taps were in the arc of admission, and the other two were in the inactive region. Turbine-inlet static pressure p_1 was measured with two taps 180° apart in the turbine inlet collector. Turbine-outlet static pressure p_5 was measured with two taps 180° apart in the outlet collector.

Shaft torque was determined with a strain-gage load cell. The load cell was used to measure the force exerted by a 10-inch (25.4-cm) torque arm mounted on the airbrake casing. The casing was cradled on air bearings.

The equipment for measuring rotative speed consisted of a six-tooth sprocket mounted on the coupling, a proximity probe, and an electronic counter.

The turbine rotative losses were experimentally determined. These losses consisted of (1) bearing and coupling windage losses and (2) rotor disk windage and pumping losses. The bearing and coupling windage torque was assumed to be a function of rotative speed only. The disk windage and pumping torque varied with both rotative speed and rotor-cavity gas density. These torque values were obtained by motoring the shaft over a range of rotative speeds and rotor-cavity gas densities. The bearing and coupling torque was obtained by determining the total torque at zero rotor-cavity density at any given speed. The disk windage and pumping torque was then determined by subtracting the bearing and coupling torque from the total torque obtained for the various values of rotor-cavity density. Bearing and coupling windage torque varied approximately with the 1.5 power of rotative speed. This bearing and coupling windage torque was added to the torque measured during tests to obtain aerodynamic torque. At design speed, bearing and coupling windage torque was 0.83 in.-lb (9.4 cm-N), which is approximately 40 percent of aerodynamic torque for 12 percent admission.

The turbine was operated at inlet conditions of 25 psia (17.24 N/cm^2 abs) and 540° R (300 K). The experimental data were obtained at inlet-static- to outlet-static-pressure ratios p_1/p_5 of 3.0 and 3.5. Full admission data were also obtained at a pressure ratio of 2.5. These static-pressure ratios are essentially equal to the stator-inlet-total- to rotor-outlet-static-pressure ratios p'_2/p_4. At each pressure ratio, the turbine speed was varied from 17 500 to 27 500 rpm in 2500-rpm increments and from 27 500 to 32 500 rpm in 1000-rpm increments. Design equivalent speed $N/\sqrt{\theta_{cr}}$ was 30 000.

RESULTS AND DISCUSSION

The results of the cold-air investigation of the 3.75-inch (9.52-cm) mean-diameter single-stage turbine at admission values of 100, 51, 31, and 12 percent are presented in terms of overall performance, partial admission losses, and variation in stator-outlet pressure.

Overall Performance

Equivalent weight flow. - The equivalent weight flow was independent of turbine pressure ratio and speed, which indicates that the stator was choked for all test conditions. The experimentally determined values of equivalent weight flow were all within the range 0.187 F to 0.188 F. For 31.37 percent admission, equivalent weight flow was 0.0588, which compares well with the design value. When the design value of 0.060 was corrected to the actual throat area, a value of 0.0587 was obtained.

Static efficiency. - The overall total to static efficiency of the subject turbine is presented in figure 5 as a function of blade-jet speed ratio ν with percent admission and overall inlet-static- to outlet-static-pressure ratio p_1/p_5 as independent variables. Figure 5 shows that, as the admission value was decreased, there was a general decrease in efficiency. At design blade-jet speed ratio of 0.377 and a static-pressure ratio of 3.0, the efficiency decreased from 0.68 to 0.56 as the arc of admission was decreased from 100 to 12 percent.

The blade-jet speed ratio for peak efficiency also decreased with the arc of admission. This decrease occurred because partial admission loss is a function of blade-jet speed ratio as well as of the arc of admission (see appendix B). For a given overall pressure ratio, a reduction in the arc of admission will cause an increase in pumping and windage loss which is proportional to the third power of the blade-jet speed ratio. The blade-jet speed ratio for peak efficiency will decrease to that value which minimizes the sum of the normal and partial admission losses.

Figure 5 also shows that for full admission there was a general decrease in efficiency as the pressure ratio was increased from 2.5 to 3.5. Stator-outlet pressure data indicate that the rotor became choked at a pressure ratio between 2.5 and 3.0. Figure 6 shows the variation of stator-outlet pressure with turbine overall pressure ratio at a blade-jet speed ratio of 0.35 for 31 and 100 percent admissions. The zero slope of the full admission curve at pressure ratios of 3.0 and 3.5 is an indication of rotor choking. When the overall pressure ratio was increased from 2.5 to 3.0, a 1 point drop in efficiency resulted. This decrease may be the result of supersonic expansion due to the divergent passage. An additional 1 point drop in efficiency occurred as the pressure ratio

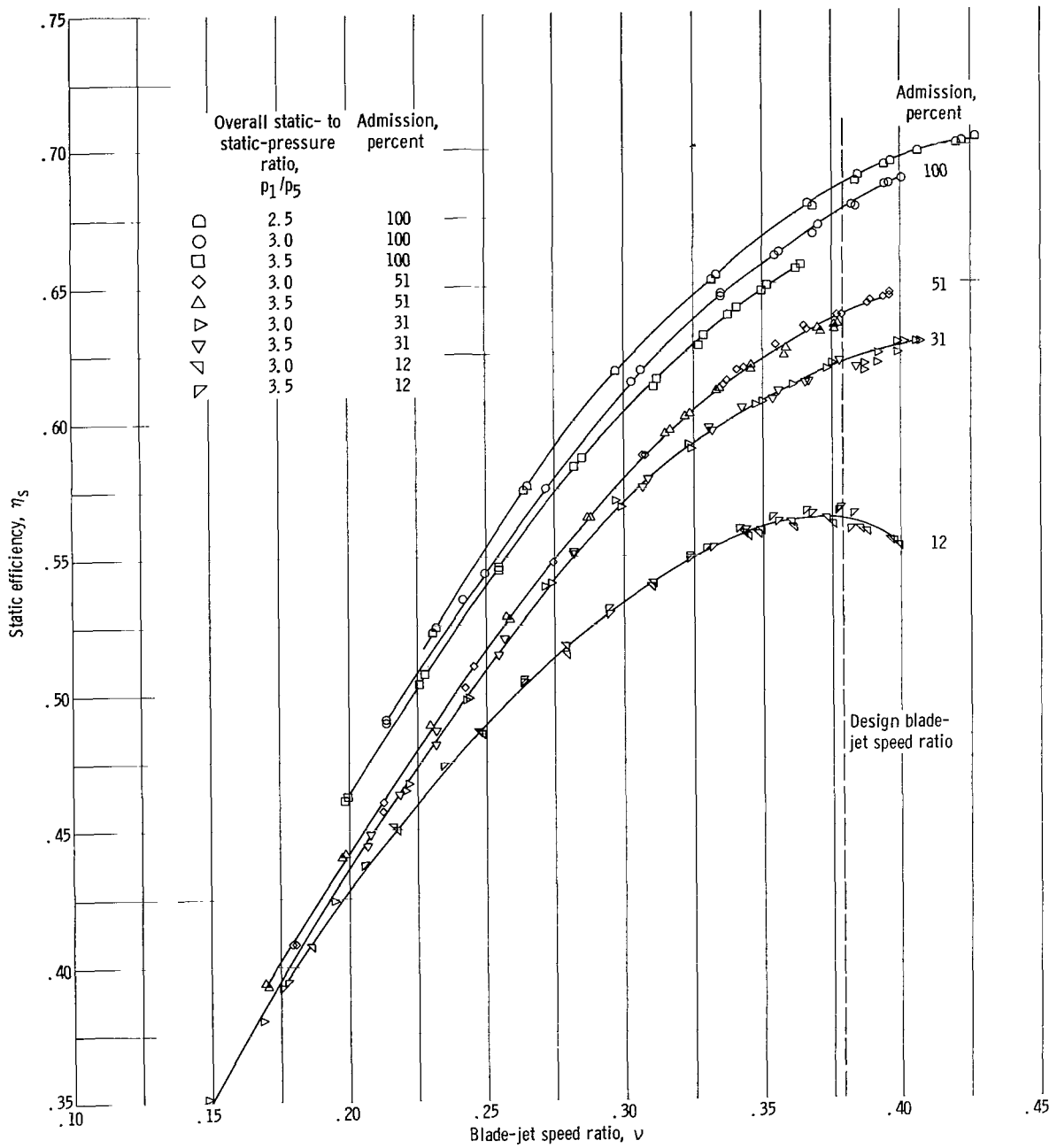

Figure 5. - Turbine efficiency characteristics.

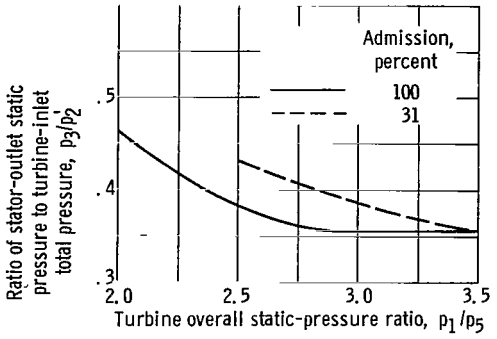

Figure 6. - Variation of stator-outlet static pressure with turbine overall static-pressure ratio. Blade-jet speed ratio, 0.35.

was increased from 3.0 to 3.5. Rotor choking did not occur during partial admission operation, possibly because of leakage into the clearance space between the stator and rotor.

Partial Admission Losses

For the following discussion, losses arising from operation with partial admission are divided into two classes, rotor pumping and windage losses and other losses. Rotor pumping and windage loss is defined as the efficiency decrease resulting from power consumption by the pumping action of the rotor blades and the disk windage. Other losses are leakage losses and losses occurring at the edge of the active arc, such as scavenging losses. As discussed in the section APPARATUS, INSTRUMENTATION, AND PROCEDURE, rotor blade pumping and disk windage torque was determined experimentally. The data thus obtained are described in appendix B, where the rotor pumping and windage torque was found to be approximated by the following equation:

$$\Gamma_{pw} = 8.4\times10^{-9}\,\rho_{av}N^2 \qquad \text{(B2)}$$

$$\Gamma_{pw} = 5.9\times10^{-9}\,\rho_{av}N^2, \text{ in SI units}$$

The torque absorbed due to rotor pumping during partial admission operation is assumed in appendix B to be proportional to the fraction of inactive annulus (1 - F). The rotor blade pumping and windage efficiency loss as derived in the appendix is described by the following equation:

$$L_{pw} = 5.6\times10^{-5}\,\rho_{av}N\nu^2\left(\frac{1-F}{F}\right) \tag{B9}$$

$$L_{pw} = 3.5\times10^{-6}\,\rho_{av}N\nu^2\left(\frac{1-F}{F}\right), \text{ in SI units}$$

Rotor pumping losses obtained from this equation for the three arcs of admission investigated herein are presented in figure 7 as a function of blade-jet speed ratio, pressure ratio, and percentage of admission. At the design blade-jet speed ratio of 0.377 and overall total- to static-pressure ratio of 3.0, the rotor pumping loss varied from 1.1 to 8.2 efficiency points as the arc of admission was reduced from 51 to 12 percent. The large increase in loss results from an increase in the term (1 - F)/F from 0.962 to 7.50. As turbine pressure ratio was increased from 3.0 to 3.5, the pumping loss de-

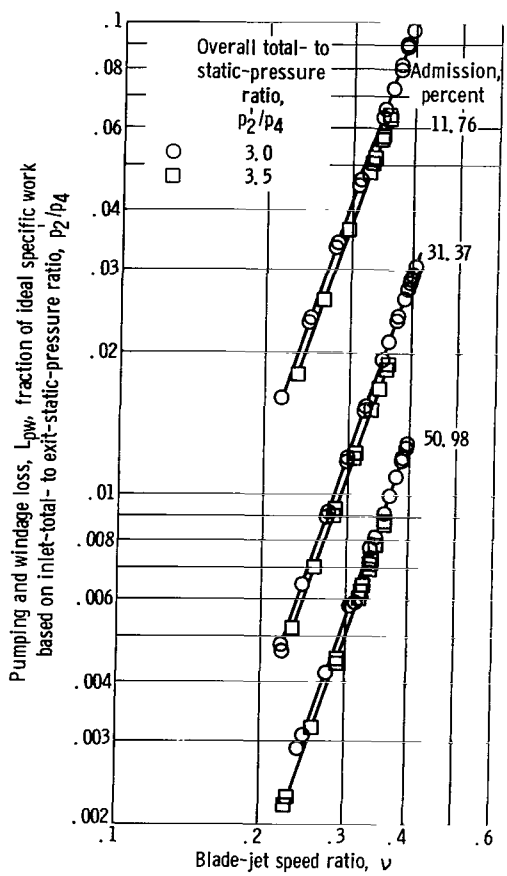

Figure 7. - Variation of pumping and windage loss with blade-jet speed ratio and percentage of admission.

creased slightly because of lower density in the rotor cavity associated with increased pressure ratio.

The total efficiency loss due to partial admission operation was obtained by subtracting the partial admission efficiency from full admission efficiency at a given blade-jet speed ratio. In the section Overall Performance, it was pointed out that at full admission rotor choking losses occur at pressure ratios of 3.0 and 3.5, but not at 2.5. It was also stated that choking does not occur during partial admission operation. In order to compare full and partial admission efficiencies on the same basis, total partial admission loss computations were based on the efficiency obtained with full admission at a pressure ratio of 2.5.

Rotor pumping and windage loss was subtracted from total loss to obtain the partial admission loss due to other factors. Figure 8 presents the variation in rotor pumping

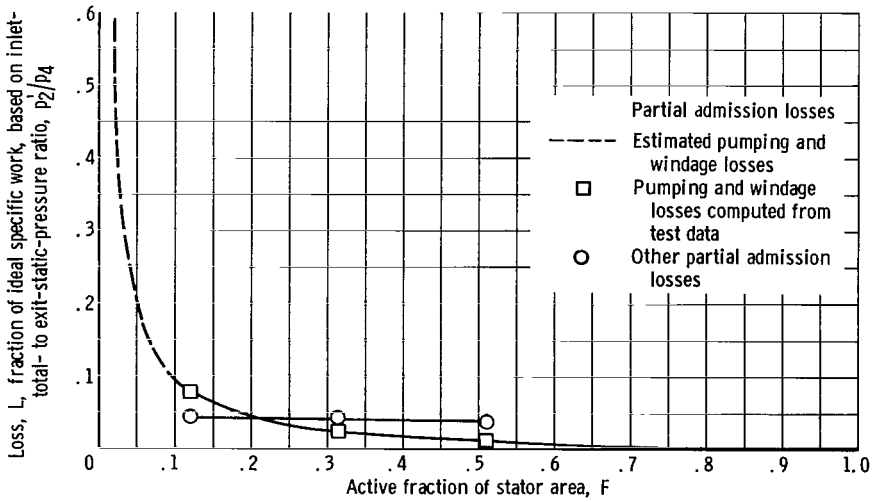

Figure 8. - Variation of computed pumping and windage losses and other partial admission losses with active fraction of stator area. Overall total- to static-pressure ratio, 3.0; blade-jet speed ratio, 0.377.

and windage loss, as well as these other losses, with percentage of admission for an overall total- to static-pressure ratio of 3.0 and a blade-jet speed ratio of 0.377. The rotor blade pumping and windage loss has been estimated for the range of 12 to 2 percent admission by assuming that the average gas density at the rotor is the same as for the 12 percent tests. In figure 8 it is shown that all other partial admission losses were essentially constant and represented approximately 4 efficiency points. These other losses were also essentially constant at values of blade-jet speed ratio above 0.25, regardless of pressure ratio or percentage of admission.

Variations in Stator Outlet Pressure

Figure 9 shows the circumferential variation of stator discharge pressure. Stator-outlet pressure p_3 is plotted as a ratio to inlet total pressure p_2' for an overall total-to static-pressure ratio of 3.0 and a blade-jet speed ratio of 0.375. The location of the six pressure taps is shown with respect to the arc of admission for the three partial admission tests.

The data for 51 and 31 percent admission show that stator-outlet pressures were

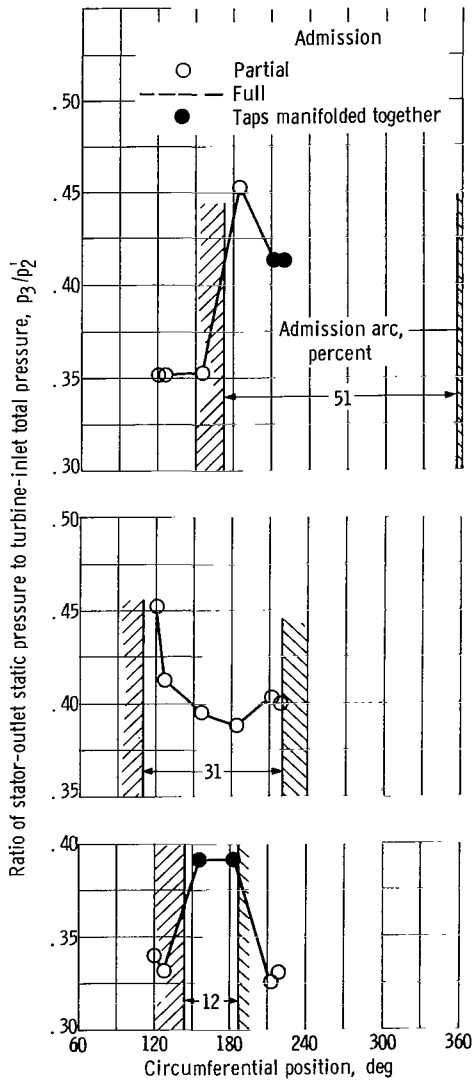

Figure 9. - Circumferential variation of stator pressure ratio. Total- to static-pressure ratio, 3.0; blade-jet speed ratio, 0.375.

highest at the edge of the active arc where the rotor blades first enter the stator jet. This effect is not apparent in the 12 percent data because the two taps in the active arc are manifolded together. These high pressures may be caused by scavenging losses. Scavenging losses are mixing losses which occur when the stator jet mixes with the relatively stagnant air in the rotor passages which are entering the active arc.

For the 51 percent admission test, there was a static-pressure drop across the inactive portion of the rotor. The average stator pressure ratio for the inactive arc was 0.352, while the turbine overall outlet-static- to inlet-total-pressure ratio was 0.333. This pressure drop indicates that there was some flow through the inactive portion of the rotor. This flow could be caused by leakage from the stator jet into the clearance space between the stator and the rotor. For the 12 percent admission test, the average stator pressure ratio was close to the turbine overall pressure ratio, which was to be expected because the leakage flow per unit area had decreased.

SUMMARY OF RESULTS

The performance of a 3.75-inch (9.52-cm) mean-diameter turbine was experimentally investigated in cold air. Performance was obtained for admission values of 100, 51, 31, and 12 percent. Partial admission losses were broken down into rotor pumping losses and all other partial admission losses. The results are summarized as follows:

1. At approximately design blade-jet speed ratio, the static efficiency decreased from 0.68 to 0.56 as admission was reduced from 100 to 12 percent.

2. From the assumption that rotor pumping and windage losses are proportional to the percentage of inactive arc, all other partial admission losses were determined to be essentially constant. These other losses were approximately 4 efficiency points for all test conditions.

3. Stator discharge pressures were highest at the edge of the arc of admission where the rotor blades first enter the active flow area. These high pressures may have been caused by scavenging losses.

Lewis Research Center,
National Aeronautics and Space Administration,
Cleveland, Ohio, April 24, 1968,
128-31-02-25-22.

APPENDIX A

SYMBOLS

F	active fraction of nozzle arc
g	conversion factor, 32.17 $\frac{\text{(lb mass)(ft)}}{\text{(lb force)(sec}^2\text{)}}$
Δh	specific-work output, Btu/lb; joule/g
Δh_{pw}	specific-work loss due to power absorbed by rotor pumping and windage action, Btu/lb; joule/g
J	mechanical equivalent of heat, 778 ft-lb/Btu
L_{pw}	static efficiency loss due to power absorbed by rotor pumping and windage action
N	rotative speed, rpm
p	absolute pressure, psia; N/cm^2 abs
R	rotor reaction, $1 - (W_3/W_4)$
U_m	mean blade velocity, ft/sec; m/sec
V	absolute gas velocity, ft/sec; m/sec
V^*_{cr}	critical velocity at U.S. standard atmosphere sea-level conditions, 1019 ft/sec; 310.6 m/sec
W	relative gas velocity, ft/sec; m/sec
w	weight flow, lb/sec; kg/sec
Γ	torque, in.-lb; cm-N
Γ_{pw}	torque output loss due to rotor pumping and windage action, in.-lb; cm-N
γ	ratio of specific heats
δ	ratio of inlet total pressure to U.S. standard atmosphere sea-level pressure, p'_2/p^*
ϵ	function of γ used in relating weight flow to that using inlet conditions at U.S. standard sea-level atmosphere, $0.740/\sqrt{\gamma\left[(\gamma+1)/2\right]^{\gamma/(\gamma-1)}}$
η_s	static efficiency, ratio of actual specific-work output to ideal specific-work output based on ratio of exit static to inlet total pressure, p_4/p'_2

θ_{cr} squared ratio of critical velocity at turbine inlet to critical velocity at U.S. standard atmosphere sea-level temperature, $\left(V_{cr,1}/V^*_{cr}\right)^2$

λ speed-work parameter, $U_m/\Delta V_u$

ν blade-jet speed ratio; $U_m/\sqrt{2gJ\,\Delta h_{id}}$; $U_m/\sqrt{2\,\Delta h_{id}}$

ρ gas density, lb/ft^3; kg/m^3

ω angular velocity, rad/sec

Subscripts:

av average

cr conditions at Mach 1

id ideal, based on total- to static-pressure ratio

u tangential direction

x axial direction

1 station at turbine-inlet collector

2 station at stator inlet

3 station between stator and rotor

4 station downstream from rotor

5 station at turbine-exit collector

Superscripts:

(') absolute total state

(*) U.S. standard conditions (temperature, 518.7° R (288.2 K); pressure, 14.70 psia (10.14 N/cm^2 abs)

APPENDIX B

DERIVATION OF EXPRESSION FOR ROTOR PUMPING AND WINDAGE LOSS

Reference 1 states that the power consumption due to disk windage and rotor pumping with no flow through the turbine can be computed from an equation of the form:

$$\text{Power} \sim \rho N^3$$

Consequently, the pumping and windage torque can be described by an equation of the form:

$$\Gamma_{pw} \sim \rho N^2 \tag{B1}$$

As indicated in the section APPARATUS, INSTRUMENTATION, AND PROCEDURE, the windage and pumping power loss was determined for the subject turbine. These data are presented in figure 10 where the ratio of disk windage and pumping torque to density Γ_{pw}/ρ is plotted as a function of the square of the rotative speed N^2. The results shown in the figure confirm the form shown in equation (B1) with the final relation as follows:

$$\Gamma_{pw} = 8.4\times10^{-9}\ \rho N^2 \tag{B2}$$

$$\Gamma_{pw} = 5.9\times10^{-9}\ \rho N^2, \text{ in SI units}$$

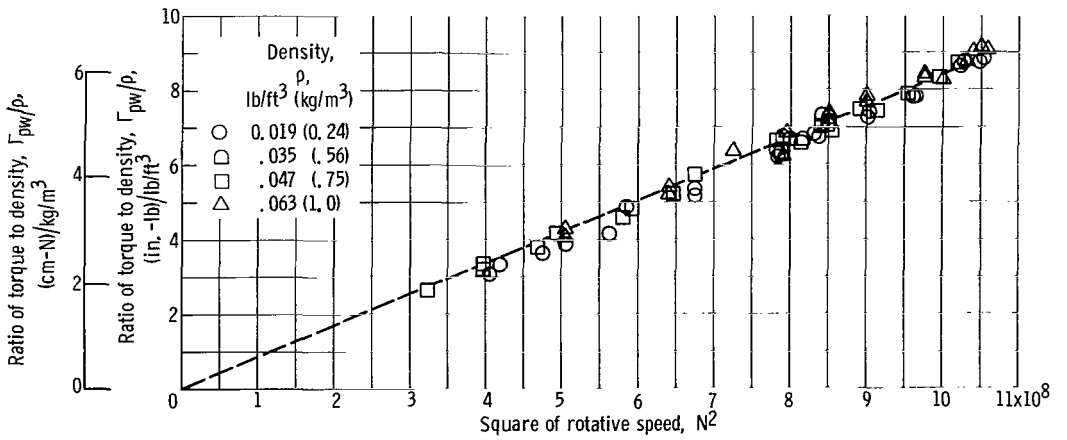

Figure 10. - Correlation of torque due to windage and pumping with rotative speed.

During partial admission operation, the disk windage torque for the inactive fraction of the arc of admission (1 - F), represents an extra loss due to partial admission operation. The disk windage torque for the active portion F represents normal windage loss equal to the windage loss for 100 percent admission. If it is assumed that pumping loss is also proportional to the inactive fraction of the arc of admission (1 - F),

$$\Gamma_{pw} \sim (1 - F)\rho N^2 \tag{B3}$$

The specific-work loss due to rotor pumping and windage Δh_{pw} is computed from the angular velocity ω, weight flow w, and the pumping and windage torque Γ_{pw} as follows:

$$\Delta h_{pw} = \frac{\Gamma_{pw}\omega}{12wJ} \tag{B4}$$

$$\Delta h_{pw} = \frac{\Gamma_{pw}\omega \times 10^{-5}}{w}, \text{ in SI units}$$

Since $w = 0.1047\ N$,

$$\Delta h_{pw} = \frac{9.41 \times 10^{-14} \rho_{av} N^3 (1 - F)}{w} \tag{B5}$$

$$\Delta h_{pw} = \frac{6.20 \times 10^{-15} \rho_{av} N^3 (1 - F)}{w}, \text{ in SI units}$$

The pumping loss L_{pw} is expressed as a fraction of ideal specific work:

$$L_{pw} = \frac{\Delta h_{pw}}{\Delta h_{id}} \tag{B6}$$

The blade-jet speed ratio is a function of N and Δh_{id}:

$$\nu = \frac{U_m}{\sqrt{2gJ\,\Delta h_{id}}} = \frac{7.31\times10^{-5}\,N}{\sqrt{\Delta h_{id}}} \qquad \text{(B7)}$$

$$= \frac{1.12\times10^{-4}\,N}{\sqrt{\Delta h_{id}}}, \text{ in SI units}$$

When equations (B5) and (B7) are substituted into equation (B6), the pumping and windage loss becomes

$$L_{pw} = \frac{1.76\times10^{-5}\,\nu^2\rho_{av}N(1 - F)}{w} \qquad \text{(B8)}$$

$$L_{pw} = \frac{4.96\times10^{-7}\,\nu^2\rho_{av}N(1 - F)}{w}, \text{ in SI units}$$

With a choked stator, the equivalent weight flow $\epsilon w\sqrt{\theta_{cr}}/\delta$ is proportional to the active fraction of stator area F. At a turbine-inlet temperature of 540° R (300 K) and an inlet total pressure of 25 psia (17.3 N/cm^2 abs), w = 0.312 F (w = 0.142 F, SI units). Using this value of weight flow in equation (B8), results in the final equation for pumping and windage loss:

$$L_{pw} = 5.6\times10^{-5}\,\nu^2\rho_{av}N\left(\frac{1 - F}{F}\right) \qquad \text{(B9)}$$

$$L_{pw} = 3.5\times10^{-6}\,\nu^2\rho_{av}N\left(\frac{1 - F}{F}\right), \text{ in SI units}$$

REFERENCE

1. Stodola, A.: Steam and Gas Turbines. Vol. 1. McGraw-Hill Book Co., Inc., 1927, p. 200.

"The aeronautical and space activities of the United States shall be conducted so as to contribute . . . to the expansion of human knowledge of phenomena in the atmosphere and space. The Administration shall provide for the widest practicable and appropriate dissemination of information concerning its activities and the results thereof."

—NATIONAL AERONAUTICS AND SPACE ACT OF 1958

NASA SCIENTIFIC AND TECHNICAL PUBLICATIONS

TECHNICAL REPORTS: Scientific and technical information considered important, complete, and a lasting contribution to existing knowledge.

TECHNICAL NOTES: Information less broad in scope but nevertheless of importance as a contribution to existing knowledge.

TECHNICAL MEMORANDUMS: Information receiving limited distribution because of preliminary data, security classification, or other reasons.

CONTRACTOR REPORTS: Scientific and technical information generated under a NASA contract or grant and considered an important contribution to existing knowledge.

TECHNICAL TRANSLATIONS: Information published in a foreign language considered to merit NASA distribution in English.

SPECIAL PUBLICATIONS: Information derived from or of value to NASA activities. Publications include conference proceedings, monographs, data compilations, handbooks, sourcebooks, and special bibliographies.

TECHNOLOGY UTILIZATION PUBLICATIONS: Information on technology used by NASA that may be of particular interest in commercial and other non-aerospace applications. Publications include Tech Briefs, Technology Utilization Reports and Notes, and Technology Surveys.

Details on the availability of these publications may be obtained from:

SCIENTIFIC AND TECHNICAL INFORMATION DIVISION

NATIONAL AERONAUTICS AND SPACE ADMINISTRATION

Washington, D.C. 20546